

# Integer Quantum Hall Effect in a Lattice Model Revisited: Kubo Formalism

Paramita Dutta,<sup>1,\*</sup> Santanu K. Maiti,<sup>2,†</sup> and S. N. Karmakar<sup>1,‡</sup>

<sup>1</sup>*Theoretical Condensed Matter Physics Division, Saha Institute of Nuclear Physics,  
Sector-I, Block-AF, Bidhannagar, Kolkata-700 064, India*

<sup>2</sup>*School of Chemistry, Tel Aviv University, Ramat-Aviv, Tel Aviv-69978, Israel*

We investigate numerically the integer quantum Hall effect (IQHE) in a two-dimensional square lattice with non-interacting electrons in presence of disorder and subjected to uniform magnetic field in a direction perpendicular to the lattice plane. We employ nearest-neighbor tight-binding Hamiltonian to describe the system, and obtain the longitudinal and transverse conductivities using Kubo formalism. The interplay between the magnetic field and disorder is also discussed. Our analysis may be helpful in studying IQHE in any discrete lattice model.

PACS numbers: 73.43.-f, 73.43.Cd

## I. INTRODUCTION

The discovery of quantum Hall effect in two-dimensional (2D) electron systems<sup>1,2</sup> exposed to strong perpendicular magnetic field was a triumph of experimental physics. Immediately after this discovery scientists from various disciplines were launched into a frenzy of activity to understand the underlying physics and also to explore its technological importance in designing different electronic devices. Such efforts have led to the endowment of a new metrological standard, the resistance quantum,  $h/e^2$ , containing two fundamental constants, the electronic charge  $e$  and the Planck's constant  $h$ <sup>3</sup>. The scaling theory of localization<sup>4</sup> suggests that in absence of magnetic field all the states of a 2D disordered non-interacting electron system are localized due to quantum interference. The time reversal symmetry is broken in the presence of magnetic field and a series of Landau bands appear due to disorder. There are numerous studies in the literature on the localisation problem of the Landau levels<sup>5,6</sup>, specifically studies based on percolation theory<sup>7</sup> and the calculation of Thouless number<sup>8</sup>. Within each Landau band a central region of extended states is flanked on both sides by regions of localized states. For a disordered 2D electron gas it is now well-understood that central region of extended states play a significant role towards the quantization of Hall conductance. In the limit of strong disorder or weak magnetic field extended states in the Landau bands float up in energy<sup>9,10</sup>, and, a systematic float-up results a transition from integer quantum Hall effect states to insulator one<sup>11</sup>.

The interplay between magnetic field and disorder is an essential issue for the phenomenon of IQHE. Breaking of translational invariance by impurity potential carries an essential need for the quantization of electronic conductivity in presence of magnetic field since in absence of disorder no plateau-like structure appears in the Hall conductivity, and the classical Hall result is preserved. Appearance of Hall plateaux is independent of physical dimension of the sample and this universality of the quantum Hall phenomenon helps the technological progress of semiconductor physics using 2D electron gas. Not only

that, the shape of the system is irrelevant in this context. With tremendous experimental successes, the phenomenon of IQHE has drawn a lot of interest among theoreticians too. Most of the theoretical studies available

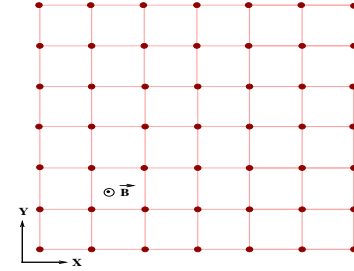


FIG. 1: (Color online). Schematic diagram of a square lattice subjected to a perpendicular magnetic field  $\mathbf{B}$ .

in the literature are based on the continuum model, ignoring the underlying lattice structure of the sample, to explain this phenomenon of IQHE. Although there are a few attempts based on discrete lattice model<sup>12–16</sup>, but a comprehensive study of this phenomenon with the framework of the lattice model is still lacking. In the present article we have made an attempt in this direction and study in details the behavior of IQHE in a square lattice in presence of disorder and address several important issues.

With this introductory remarks we organize this paper as follows. In section II we describe the model and theoretical technique for the calculation of longitudinal and transverse conductivities based on Kubo formalism. The numerical results and discussion are included in section III. Finally, we draw our conclusions in section IV.

## II. MODEL AND THEORETICAL FORMULATION

### A. The Model

We start with a 2D square lattice (Fig. 1) which contains  $N_x$  and  $N_y$  number of atomic sites along the  $x$ - and

$y$ -directions, respectively and subject it to a perpendicular magnetic field  $\mathbf{B}$ . We employ a tight-binding (TB) Hamiltonian to describe the system, and, under nearest-neighbor hopping approximation it reads as,

$$\mathbf{H} = \sum_{m,n} \epsilon_{m,n} c_{m,n}^\dagger c_{m,n} + t \sum_{m,n} \left( c_{m+1,n}^\dagger c_{m,n} + c_{m,n+1}^\dagger c_{m,n} e^{i\theta_m} + \text{h.c.} \right) \quad (1)$$

where,  $\epsilon_{m,n}$  denotes the site energy of an electron at site  $(m,n)$ ,  $m$  and  $n$  being the  $x$  and  $y$  co-ordinates of the site, respectively (setting lattice constant  $a = 1$ ). In order to incorporate impurities in the sample, we choose site energies  $\epsilon_{m,n}$  randomly from a ‘Box’ distribution function of width  $W$ . Here,  $t$  is the hopping integral between the neighboring sites either along  $x$ - or  $y$ -direction and  $c_{m,n}^\dagger$  ( $c_{m,n}$ ) is the creation (annihilation) operator of an electron at the site  $(m,n)$ . In the presence of magnetic field  $\mathbf{B}$ , a phase factor  $\theta_m$  is introduced into the above

Hamiltonian (Eq. 1) and for a particular choice of gauge  $\mathbf{A} = (0, Bx)$ , the so-called Landau gauge, it becomes non-zero only when an electron moves along the  $y$  direction. Then this phase factor can be expressed as  $\theta_m = 2\pi m\phi$ , where  $\phi$  is the magnetic flux per plaquette measured in units of the elementary flux-quantum  $\phi_0 = ch/e$ . We set  $\phi = 1/Q$ , where  $Q$  is an integer and the choice of  $Q$  should be such that it is commensurate with  $N_y$ . This reduces the boundary conditions to the traditional periodic ones<sup>17</sup>.

## B. Linear Response Kubo Formalism

To obtain the longitudinal and transverse conductivities, we use the Kubo formalism which is briefly outlined below. The general expression for electrical conductivity is written in the form,

$$\sigma_{kl} = \frac{ie^2\hbar}{N} \sum_{\alpha} \sum_{\beta \neq \alpha} (f_{\alpha} - f_{\beta}) \frac{\langle \alpha | \dot{\mathbf{u}}_k | \beta \rangle \langle \beta | \dot{\mathbf{u}}_l | \alpha \rangle}{(\mathcal{E}_{\alpha} - \mathcal{E}_{\beta})^2 + \eta^2} + \frac{e^2\hbar}{N} \sum_{\alpha} \sum_{\beta \neq \alpha} \left( \frac{f_{\alpha} - f_{\beta}}{\mathcal{E}_{\alpha} - \mathcal{E}_{\beta}} \right) \frac{\eta}{(\mathcal{E}_{\alpha} - \mathcal{E}_{\beta})^2 + \eta^2} \langle \alpha | \dot{\mathbf{u}}_k | \beta \rangle \langle \beta | \dot{\mathbf{u}}_l | \alpha \rangle \quad (2)$$

where,  $\eta \rightarrow 0^+$ . Here, the indices  $k$  and  $l$  can be  $x$  or  $y$ . For  $k = l = x$ , we get  $\sigma_{xx}$ , the so-called longitudinal conductivity while for the other case we have the transverse conductivity,  $\sigma_{xy}$ . The states  $|\alpha\rangle$  and  $|\beta\rangle$  are the eigenstates of the Hamiltonian (Eq. 1) corresponding to the energy eigenvalues  $\mathcal{E}_{\alpha}$  and  $\mathcal{E}_{\beta}$ , respectively, and  $N = N_x \times N_y$  represents the size of the sample.  $\dot{\mathbf{u}}_k$  is the velocity operator along  $k$ -th ( $x$  or  $y$ ) direction and  $f_{\alpha(\beta)} = 1/[1 + \text{Exp}\{(\mathcal{E}_{\alpha(\beta)} - E_F)/k_B T\}]$  is the Fermi distribution function at absolute temperature  $T$  with Fermi energy  $E_F$ .

When  $k$  and  $l$  are identical to each other, the factor  $\langle \alpha | \dot{\mathbf{u}}_k | \beta \rangle \langle \beta | \dot{\mathbf{u}}_l | \alpha \rangle$  in Eq. 2 becomes a real and positive one, while it becomes purely imaginary when  $k$  and  $l$  are different. Since the conductivity is a real and positive quantity, the first term on the right hand side of Eq. 2 gives transverse conductivity ( $\sigma_{xy}$ ), while the second term represents longitudinal conductivity ( $\sigma_{xx}$ ). Separating the transverse and longitudinal parts we can write,

$$\sigma_{xy} = \frac{ie^2\hbar}{N} \sum_{\alpha} \sum_{\beta \neq \alpha} (f_{\alpha} - f_{\beta}) \frac{\langle \alpha | \dot{\mathbf{u}}_x | \beta \rangle \langle \beta | \dot{\mathbf{u}}_y | \alpha \rangle}{(\mathcal{E}_{\alpha} - \mathcal{E}_{\beta})^2 + \eta^2} \quad (3)$$

and

$$\sigma_{xx} = \frac{e^2\hbar}{N} \sum_{\alpha} \sum_{\beta \neq \alpha} \left( \frac{f_{\alpha} - f_{\beta}}{\mathcal{E}_{\alpha} - \mathcal{E}_{\beta}} \right) \frac{\eta}{(\mathcal{E}_{\alpha} - \mathcal{E}_{\beta})^2 + \eta^2} |\langle \alpha | \dot{\mathbf{u}}_x | \beta \rangle|^2. \quad (4)$$

### • Matrix elements of the Velocity operators:

To calculate the matrix elements of the velocity operators  $\dot{\mathbf{u}}_k$  we start with the basic relation<sup>18</sup>,

$$\dot{\mathbf{u}}_k = \frac{1}{i\hbar} [\mathbf{u}_k, \mathbf{H}] \quad (5)$$

where,  $\mathbf{u}_k$  is the displacement operator along  $k$ -th ( $x$  or  $y$ ) direction and  $\mathbf{H}$  is the Hamiltonian operator described in Eq. 1. Expanding and simplifying the above relation (Eq. 5) we get the velocity operators in the following second quantized form along the  $x$ - and  $y$ -directions,

$$\dot{\mathbf{u}}_x = \frac{it}{\hbar} \sum_{m,n} \left( c_{m,n}^\dagger c_{m+1,n} - c_{m+1,n}^\dagger c_{m,n} \right) \quad (6)$$

and,

$$\dot{\mathbf{u}}_y = \frac{it}{\hbar} \sum_{m,n} \left( c_{m,n}^\dagger c_{m,n+1} e^{-i\theta_m} - c_{m,n+1}^\dagger c_{m,n} e^{i\theta_m} \right). \quad (7)$$

Therefore, the textcoloredmatrix elements of the velocity operators with respect to the eigenvectors  $|\alpha\rangle$  and  $|\beta\rangle$  become,

$$\langle \alpha | \dot{\mathbf{u}}_x | \beta \rangle = \frac{it}{\hbar} \sum_{m,n} \left( a_{m,n}^{\alpha*} a_{m+1,n}^{\beta} - a_{m+1,n}^{\alpha*} a_{m,n}^{\beta} \right) \quad (8)$$

and,

$$\langle \alpha | \dot{\mathbf{u}}_y | \beta \rangle = \frac{it}{\hbar} \sum_{m,n} \left( a_{m,n}^{\alpha*} a_{m,n+1}^{\beta} e^{-i\theta_m} - a_{m,n+1}^{\alpha*} a_{m,n}^{\beta} e^{i\theta_m} \right) \quad (9)$$

where, the eigenvectors look like,

$$|\alpha\rangle = \sum_{p,q} a_{p,q}^{\alpha} |p, q\rangle \quad (10)$$

and,

$$|\beta\rangle = \sum_{p,q} a_{p,q}^{\beta} |p, q\rangle. \quad (11)$$

Here,  $|p, q\rangle$ 's are the Wannier states and  $a_{p,q}^{\alpha}$  and  $a_{p,q}^{\beta}$ 's are the corresponding coefficients. Taking the contributions from all these states we find the matrix elements of the velocity operators along the  $x$ - and  $y$ -directions.

Substituting the above expressions (Eqs. 8 and 9) into Eqs. 3 and 4 we get the relations,

$$\begin{aligned} \sigma_{xy} = & -\frac{2\pi it^2}{\hbar N} \sum_{\alpha} \sum_{\beta \neq \alpha} \frac{(f_{\alpha} - f_{\beta})}{(\mathcal{E}_{\alpha} - \mathcal{E}_{\beta})^2 + \eta^2} \\ & \times \left\{ \sum_{m,n} \left( a_{m,n}^{\alpha*} a_{m+1,n}^{\beta} - a_{m+1,n}^{\alpha*} a_{m,n}^{\beta} \right) \right\} \\ & \times \left\{ \sum_{m,n} \left( a_{m,n}^{\beta*} a_{m,n+1}^{\alpha} e^{-i\theta_m} - a_{m,n+1}^{\beta*} a_{m,n}^{\alpha} e^{i\theta_m} \right) \right\} \end{aligned} \quad (12)$$

and,

$$\begin{aligned} \sigma_{xx} = & \frac{2\pi t^2}{\hbar N} \sum_{\alpha} \sum_{\beta \neq \alpha} \left( \frac{f_{\alpha} - f_{\beta}}{\mathcal{E}_{\alpha} - \mathcal{E}_{\beta}} \right) \frac{\eta}{(\mathcal{E}_{\alpha} - \mathcal{E}_{\beta})^2 + \eta^2} \\ & \times \left| \sum_{m,n} \left( a_{m,n}^{\alpha*} a_{m+1,n}^{\beta} - a_{m+1,n}^{\alpha*} a_{m,n}^{\beta} \right) \right|^2. \end{aligned} \quad (13)$$

These are the final expressions for the transverse and longitudinal conductivities, respectively, which offer a very convenient method for numerical calculation of the conductivities using Kubo formalism.

Throughout our study we choose the units where  $c = e = \hbar = 1$  and measure the energy scale in units of  $t$ .

### III. NUMERICAL RESULTS AND DISCUSSION

#### A. Energy Spectrum

To make this present communication a self-contained one let us begin with the energy band structure of our model quantum system.

In Fig. 2 we present the energy levels for a finite size square lattice in presence of a transverse magnetic field

both for the ordered as well as the disordered cases. The vertical lines correspond to the locations of the energy eigenvalues. For the ordered case we use black lines, while the blue lines are used for the disordered case, and, these two colored lines are superimposed in each plot to reveal the effect of disorder clearly. In the absence of disorder we get very sharp lines associated with the energy eigenvalues of the lattice and all these energy levels are highly degenerate. The degeneracy factor of the energy levels strongly depends on the specific choice of the magnetic field, i.e., on the value of  $Q$ . When  $Q$  becomes commensurate with  $N_y$ , we get  $Q$  number of such sharp energy levels and each level becomes  $N/Q$ -fold degener-

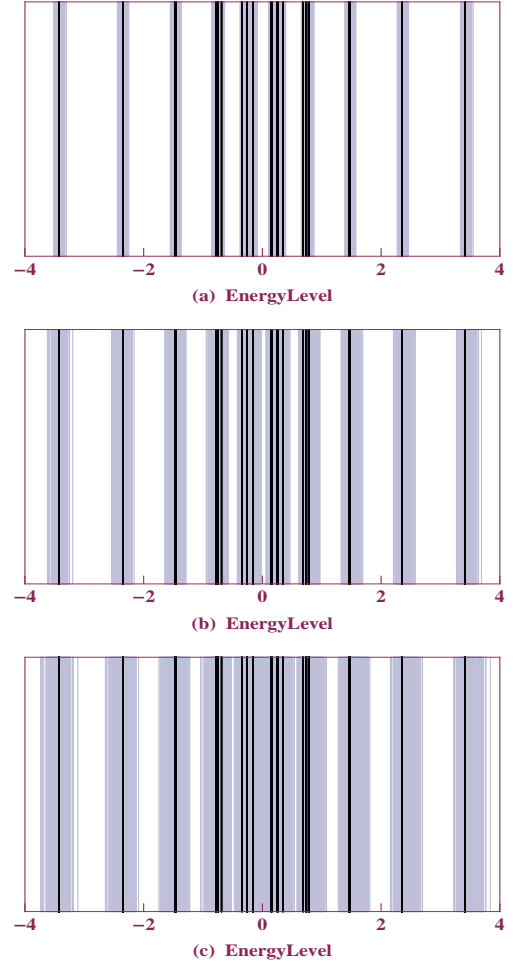


FIG. 2: (Color online). Energy levels for a square lattice ( $30 \times 30$ ) when  $\phi$  is set at 0.1. The black lines represent the locations of the energy levels for the ordered ( $W = 0$ ) case. On the other hand, the blue lines denote the positions of the energy levels for the disordered ( $W \neq 0$ ) case, where (a), (b) and (c) correspond to  $W = 1, 2$  and  $3$ , respectively.

ate. These levels are quite similar to the Landau levels of the continuum model of 2D electron gas. It is to be noted that unlike the equispaced Landau levels of the continuum model, we do not have equispaced energy levels for finite sized square lattice. The levels are widely

separated near the two edges of the energy spectrum as observed from Fig. 2. The situation is somewhat interesting when impurities are introduced into the system. In presence of disorder the degeneracy of each Landau band gets lifted due to the impurity potentials and the sharp energy levels form quasi-bands keeping the total number of energy levels in each quasi-band identical to each other and this number is equal to the degeneracy of the band. As far example, if we choose  $N_x = N_y = 30$  and set the magnetic flux  $\phi$  at 0.1 (i.e.,  $Q = 10$ ), then 10 Landau bands appear in the spectrum (Fig. 2) and each band contains 90 energy levels. The width of each Landau band increases with the increase of strength of disorder  $W$  as can be observed from the spectra, and for large enough disorder strength the neighboring Landau bands start to overlap with each other.

### B. Transverse and Longitudinal Conductivities

Let us now illustrate the characteristics features of longitudinal and transverse conductivities and the related issues for a finite sized square lattice. In Fig. 3 we show the variation of transverse conductivity  $\sigma_{xy}$  (red line) as a function of Fermi energy  $E_F$  for a  $(60 \times 60)$  square lattice considering  $\phi = 0.1$ ,  $W = 1$  and  $k_B T = 0.01$ . The Landau levels (light green) are also superimposed

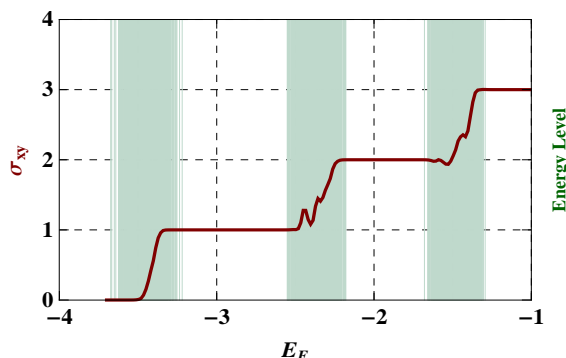


FIG. 3: (Color online). Transverse conductivity (red curve) as a function of Fermi energy for a square lattice  $(60 \times 60)$  considering  $\phi = 0.1$ ,  $W = 1$  and  $k_B T = 0.01$ . The Landau bands (light green) are superimposed on it.

on the spectrum. From the spectrum it is clear that the transverse/Hall conductivity  $\sigma_{xy}$  increases in integer steps with the rise of Fermi energy  $E_F$  and at these plateaux the Hall conductivity gets the value,  $\nu e^2/h$  with a great accuracy, where the integer number  $\nu$  corresponds to the total number of filled Landau bands below the Fermi level. For a particular system size the total number of available Hall plateaux strongly depends on the choice of magnetic flux  $\phi$ , since the specific choice of  $\phi$  fixes the total number of Landau bands as mentioned earlier. Very interestingly we observe that even for a square lattice whenever the Fermi energy crosses any one

of the Landau bands, the Hall conductivity enhances exactly by the same amount  $e^2/h$ , and accordingly, for  $\nu$  filled Landau bands,  $\sigma_{xy}$  becomes equal to  $\nu e^2/h$ , which is precisely the characteristic feature of integer quantum Hall effect. It is important to note that in traditional ballistic waveguides we also get quantized conductance, but such a strange precise quantization, about one part in million, can never be achieved in ordinary ballistic conductors as the backscattering processes are not completely suppressed. The almost complete elimination of the backscattering processes can only be obtained in the quantum Hall regime which actually ensures the extremely high precision in the quantized value of Hall conductivity. Recently, it has been reported that when the Fermi energy lies within a plateau region, there is practically zero overlap between the current carrying states in the sample leading to the almost complete suppression of

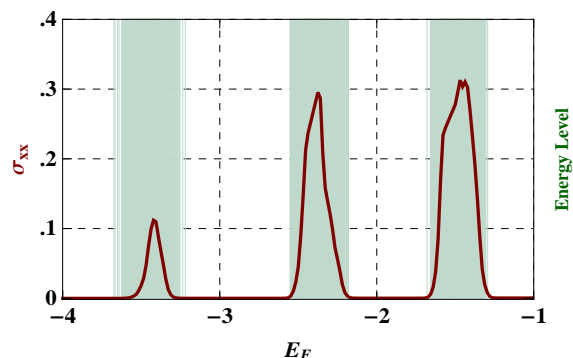


FIG. 4: (Color online). Longitudinal conductivity (red curve) as a function of Fermi energy for a square lattice  $(60 \times 60)$  for the same parameter values given in Fig. 3. The Landau bands (light green) are superimposed on it.

the backscattering processes and thereby the momentum relaxation process<sup>16</sup>.

As a result of almost entire suppression of the backscattering processes for Fermi energy lying in the plateau regions, we would get practically zero longitudinal resistance and hence vanishing longitudinal conductivity which directly follows from the conductivity tensor. The result is shown in Fig. 4 where we set the same parameter values as given in Fig. 3. The resistance of a conductor is associated with the rate at which electrons can relax their momentum. To loose the momentum an electron has to be scattered through the allowed energy eigenstates in the bulk of the conductor. This almost vanishes whenever the Fermi energy lies between two Landau bands. The longitudinal resistance is non-vanishing only when the Fermi energy is within a Landau band where the backscattering process are present.

Figure 3 clearly shows that the Hall plateaux get extended well inside the Landau bands and the Hall conductivity rises only within certain central region of each Landau bands. The underlying physics behind it as follows. In presence of disorder Landau bands get broad-

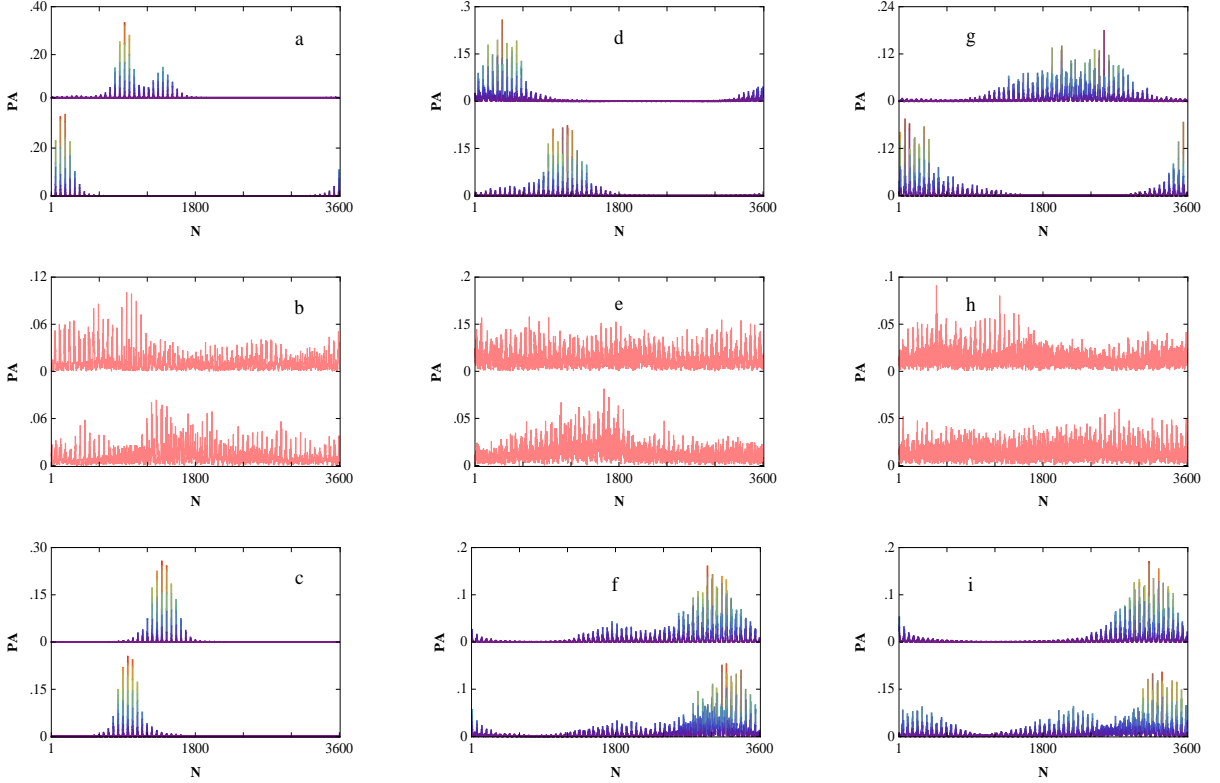


FIG. 5: (Color online). Probability amplitude (PA) at different lattice sites ( $N$ ) of a square lattice ( $60 \times 60$ ) for the same parameter values as mentioned in Fig. 3. The top and bottom panels correspond to the results for the eigenstates selected from the left and right edges of the Landau band, respectively, while the middle one is for the eigenstates lie in the centre of the Landau band. The three different columns are associated with the three different Landau bands shown in Fig. 3. To understand the nature of energy eigenstates more clearly, in each figure we present the results for two states those are chosen from the respective regions.

ened and the natures of all eigenstates in a Landau band are not identical. The states those lie along the two edges of the Landau band are localized, while the states in the middle are almost extended. To reveal the nature of the energy eigenstates whether they are quasi-localized or extended, in Fig. 5 we show the variation of probability amplitude at different lattice sites of a square lattice with the same set of parameters as those taken in Fig. 3. The top and bottom panels correspond to the energy levels chosen from the left and right edges of the three Landau bands, respectively, while the middle panel refers to some of the energy levels near the centre of the Landau bands. Quite clearly we see that near the band edges the probability amplitude vanishes almost at all sites excepting a few, which implies that electrons are localized in these states. On the other hand, for the states well inside the Landau bands we have finite probability amplitude on each site revealing the extended nature of the states. This behavior is true for every Landau band. Therefore, for the energy levels which lie near the two edges of the Landau bands we have almost zero contribution to the transverse conductivity and it leads to the plateau regions in the Hall conductivity, and, the non-zero contribution comes only from the extended states near the center of the Lan-

dau bands. We also observe that the length of the Hall plateaux get widened with the rise of impurity strength, but it does not affect the quantized nature of Hall conductance. The quantization of Hall conductance is very robust and really very surprising. This is due to the fact that when we increase the strength of disorder in the sample, more states become localized from the edges of the Landau bands and the regions of extended states in the band centre becomes narrow. However, the contribution to Hall conductivity that gets lost due to these additional localized states is exactly compensated by the enhanced contribution from the extended states, and accordingly, the quantized nature of Hall conductivity remains unaltered. This phenomenon is known as the current compensation and it has already been discussed in the literature by using the continuum model<sup>19</sup>.

### C. Effect of Magnetic Field and Temperature

So far we have discussed the main aspects of integer quantum Hall effect in a square lattice, but for the sake of completeness now we focus our attention on the effects of magnetic field and temperature on IQHE as this



phenomenon is highly sensitive to the interplay of these parameters. With the increase of disorder strength the Hall plateaux can be found to be destroyed one by one in a generic sequence<sup>12</sup>.

In Fig. 6 we present the variation of Hall conductivity of a square lattice ( $60 \times 60$ ) as a function of Fermi energy for three different values of magnetic flux  $\phi$  reg-

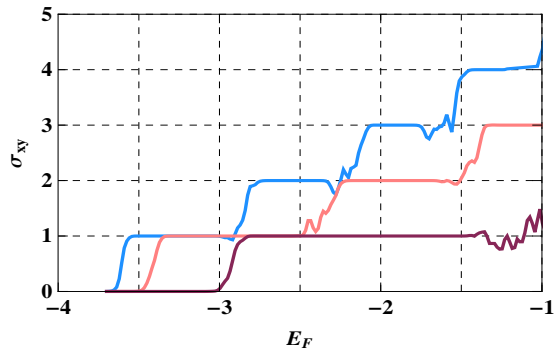


FIG. 6: (Color online). Hall conductivity as a function of Fermi energy for a square lattice ( $60 \times 60$ ) with  $W = 1$  and  $K_B T = 0.1$ . The dark-violet, pink and blue lines correspond to  $Q = 5, 10$  and  $15$ , respectively.

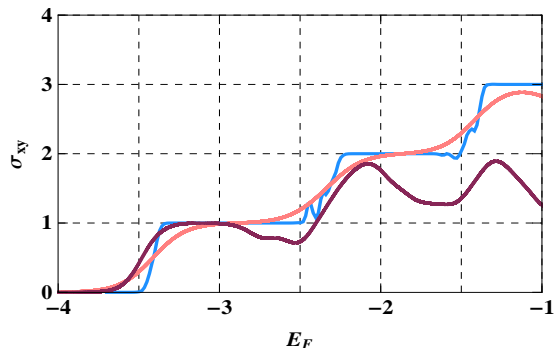


FIG. 7: (Color online). Hall conductivity as a function of Fermi energy for a square lattice ( $60 \times 60$ ) considering  $W = 1$  and  $\phi = 0.1$ . The blue, pink and dark-violet colors correspond to  $k_B T = 0.01, 0.05$ , and  $0.1$ , respectively.

ulated by the parameter  $Q$  since  $\phi = 1/Q$ . Here we set  $k_B T = 0.1$  and  $W = 1$ . The dark-violet, pink and blue curves correspond to  $Q = 5, 10$  and  $15$ , respectively, and these values of  $Q$  are such that  $N_x$  is exactly divisible by

them so that the translational invariance remains along the  $x$ -direction. For a given value of  $Q$ , we have  $Q$  Landau bands in the energy spectrum, and accordingly, for a certain energy range the number of Hall plateaux are different for various  $Q$  as can be seen clearly from Fig. 6. However, in all these cases the quantized nature of the Hall conductance is exactly maintained, i.e.,  $\sigma_{xy}$  is integer multiple of the factor  $e^2/h$  with a great accuracy.

The effect of temperature in IQHE is illustrated in Fig. 7, where we show the results for three temperatures considering  $W = 1$  and flux  $\phi = 0.1$ . For a finite disorder strength and weak magnetic field, the widths of the Hall plateaux decrease gradually with the rise of temperature and the conductance spectrum becomes quite messy. For a sufficiently large temperature the phenomenon of conductance quantization almost disappears and this phenomenon has also been verified experimentally by some groups<sup>20,21</sup>. When the Fermi level is placed anywhere within the localized regions, the thermally excited electrons can jump toward the extended region and contribute to the conductivity. Thus, there is a competition between these two issues as a result the quantization gets lost gradually.

#### IV. CONCLUSION

In conclusion, we have re-visited the phenomenon of integer quantum Hall effect in a two-dimensional square lattice within a non-interacting electron picture. The interplay between the magnetic field and randomness has been discussed in detail. We have used a single-band nearest-neighbor tight-binding Hamiltonian to describe the model quantum system and numerically calculated the longitudinal and transverse conductivities by using Kubo formalism. The physical picture about the integer quantum Hall effect that has emerged from our present investigation based on the discrete lattice model is almost the same as that obtained in the continuum model. Our approach could be much more suitable for further investigation of the Quantum Hall effect in topologically insulating materials, like, graphene flakes, kagome lattices, etc. This is our first step towards this direction.

#### V. ACKNOWLEDGMENT

We thank Shreekantha Sil for some useful discussion.

\* Electronic address: paramita.dutta@saha.ac.in

† Electronic address: santanu@post.tau.ac.il

‡ Electronic address: sachindranath.karmakar@saha.ac.in

<sup>1</sup> K. v. Klitzing, G. Dorda, and M. Pepper, Phys. Rev. Lett. **45**, 494 (1980).

<sup>2</sup> D. J. Thouless, Surf. Sci. **142**, 147 (1984).

<sup>3</sup> A. Hartland, Metrologia **29**, 175 (1992).

<sup>4</sup> E. Abrahams, P. W. Anderson, D. C. Licciardello, and T. V. Ramakrishnan, Phys. Rev. Lett. **42**, 673 (1979).

<sup>5</sup> S.-R. Eric Yang, A. H. MacDonald, and B. Huckestein, Phys. Rev. Lett. **74**, 3229 (1995).

<sup>6</sup> Y. Tan, J. Phys.: Condens. Matter **6**, 7941 (1994).

- <sup>7</sup> S. A. Trugman, Phys. Rev. B **27**, 7539 (1983).
- <sup>8</sup> T. Ando, J. Phys. Soc. Japan **52**, 1740 (1983).
- <sup>9</sup> K. Yang and R. N. Bhatt, Phys. Rev. Lett. **76**, 1316 (1996).
- <sup>10</sup> K. Yang and R. N. Bhatt, Phys. Rev. B **59**, 8144 (1999).
- <sup>11</sup> D. N. Sheng, Z. Y. Weng, and X. G. Wen, Phys. Rev. B **64**, 165317 (2001).
- <sup>12</sup> D. N. Sheng and Z. Y. Weng, Phys. Rev. Lett. **78**, 318 (1997).
- <sup>13</sup> D. N. Sheng and Z. Y. Weng, Phys. Rev. Lett. **80**, 580 (1998).
- <sup>14</sup> G. Czycholl, Solid State Commun. **67**, 499 (1988).
- <sup>15</sup> S. S. Mandal and M. Acharyya, Physica B **252**, 91 (1998).
- <sup>16</sup> S. K. Maiti, M. Dey, and S. N. Karmakar, Phys. Lett. A (in press).
- <sup>17</sup> D. N. Sheng, L. Sheng, and Z. Y. Weng, Phys. Rev. B **73**, 233406 (2006).
- <sup>18</sup> P. Dutta, S. K. Maiti, and S. N. Karmakar, Eur. Phys. J. B (in press).
- <sup>19</sup> M. Janssen and J. Hajdu, Z. Phys. B **70**, 461 (1988).
- <sup>20</sup> M. E. Cage, B. F. Field, R. F. Dziuba, S. M. Girvin, A. C. Gossard, and D. C. Tsui, Phys. Rev. B **30**, 2286(R) (1984).
- <sup>21</sup> H. P. Wei, A. M. Chang, D. C. Tsui, and M. Razeghi, Phys. Rev. B **32**, 7016(R) (1985).